zaeee

by Jurnal Jurusan Teknik Mesin Polsri

Submission date: 29-Jun-2024 01:16PM (UTC+0900)

Submission ID: 2378367261

File name: turnitin_sabtu.docx (2.37M)

Word count: 5671

Character count: 33382

Research Article

Inhibition of Acetylcholinesterase using Bioactive Compound from *Moringa* oleifera: Molecular Docking and Dynamic Studies

25 Abstract

Alzheimer's disease is a neurodegenerative disorder caused by acetylcholine hydrolysis that impairs cognitive brain function. This research aims to determine the interaction and dynamic of ligands from *Moringa oleifera* on AChE through Lipinski's Rule, ADMET properties, molecular docking calculations, and molecular dynamic simulations. Lipinski's Rule calculation provided ligand limits that adhere to druglikeness properties. ADMET results also showed that several ligands satisfy ADMET properties. Pterygospermin has lower binding energy than the ligand control (-10.28 kJ mol⁻¹) with amino acid residues of TYR133 and GLU202. It indicates a favorable interaction between the AChE receptor and ligand in the inhibition process. Based on molecular docking calculations, pterygospermine inhibits the AChE receptor at the Long, narrow aromatic gorge active site. However, this data is different from the ligand control interaction mode. Molecular dynamic investigations of the pterygospermine ligand in the complex revealed the stability and unfolded effect on the protein, although the energy of rivastigmine was higher due to conformation.

Keywords: acetylcholinesterase, molecular docking, molecular dynamic, Moringa oleifera, pterygospermine

16 1. INTRODUCTION

Alzheimer's is a neurodegenerative disorder that progressively hinders brain function in humans ¹. Alzheimer's disease is triggered by the presence of *Acetylcholinesterase* (AChE) that hydrolyzes acetylcholine into choline and acetate, disturbing the brain's neuron system ². In the absence of treatment for this disease, symptoms are susceptible to dementia. A patient with Alzheimer's exhibits traits including memory impairment, issues thinking and reasoning, diminished language, and dramatic mood fluctuations³. The alternative treatment for Alzheimer's in clinical practice commonly involves synthetic drugs like rivastigmine, donepezil, neostigmine, and tacrine^{4,5}. These drugs have been demonstrated to be effective AChE inhibitors. However, they may cause side effects such as diarrhea, vomiting, syncope, bradycardia, and nausea ⁶. These medications have modest drug performance and only reduce symptoms⁶. However, the therapeutic for alzheimer's disease in clinical practice was used as a model for creating new medications. Therefore, developing novel medicines derived from secondary metabolites of medicinal plants is critical because bioactive molecules have a broad spectrum of bioactivity ². The study of anti-alzheimer from medicinal plants is a potential future drug candidate ⁷. *Moringa oleifera* is among the medicinal herbs that suppress AChE in Alzheimer's.

Moringa oleifera is traditionally applied as a medication in society. The liquid extracted from the bark has been utilized to cure meningitis. In addition, a decoction of Moringa oleifera root has been administered to treat female hysteria and epilepsy ⁸. Moringa oleifera is a medicinal plant with rich benefits such as neuroprotective ^{9,10}, antilipase, anti-AChE ¹¹, anti-inflammatory, anti-tumor, anti-neuroinflammatory¹², anticancer, liver protection, regulate enzyme activity, modulate blood glucose, and induce cell cycle arrest, and apoptosis ¹³. Because of the fascinating benefits of Moringa oleifera, this plant has been developed as a new drug for alzheimer disease. Moringa oleifera includes secondary metabolites, notably phenolics, flavonoids, tannins, vitamin C, and alkaloids. Antioxidants in this medical plant also avert free radicals that attack nerve cells. Quercetin on extract was proven to inhibit the AChE enzyme ¹⁴. Previous studies reported that the extract of hexane solvent root revealed a high anti-AChE of 1.86 ± 0.06 mg ml⁻¹.

Furthermore, the leaf extract of *Moringa oliefera* using methanol and ethyl acetate has also proven an inhibition ability to AChE and butyrylcholinesterase (BChE) ¹⁵. Djiogue et al. (2022) also appended information that could prevent hippocampus nerve loss in test animals ¹⁰. They also claimed that this extract has neuroprotective ¹², antioxidant, and memory-protective functions ^{10,16}. An alkaloid content on *Moringa oleifera* has mitigated oxidative pressure and inflammation ¹⁷. Currently, the utilization of an in silico approach to discovery of drug is a promising field because it is efficient, fast, and inexpensive ¹⁸. As a result, the potential

of bioactive chemicals isolated from *Moringa oliefera* as AChE inhibitors was investigated using the Lipinski Rule of Five, ADMET properties, molecular docking calculation, and molecular dynamics simulation. In theory, natural and pharmaceutical researchers might utilize this data as a predictor while developing Alzheimer's therapies to reduce failure. In practice, the findings of this study could be applied to carry out additional research on *Moringa oleifera* medicinal plants.

2. RESEARCH METHODS

Lipinski's Rules of Five and ADMET Studies

Lipinski's Rule of Five aimed to evaluate bioactive compounds derived from *Moringa oliefera* as drug candidates that fulfilled the rule of drug-likeness. Bioactive compounds that adhere to Lipinski's rules have physic-chemistry properties for oral administration in humans. The rules are molecular weight ≤500 Da, the partition coefficient of octanol/water (MlogP) ≤5, Hydrogen Bond Acceptor (HBA) ≤10, and Hydrogen Bond Donor (HBD) ≤5 lipinski's Rule of Five will be calculated using a molecular docking study. Furthermore, the ADMET prediction is used to obtain the pharmacokinetics of the drug candidate from *Moringa oliefera*. The information from ADMET prediction is % Human Intestinal Absorption (HIA), Carcinoma Colon-2 (C22-2) cell, % Plasma Protein Binding (PPB), Blood blood-brain barrier (BBB), mutagen, and carcinogen 20. Lipinski's Rule of Five and ADMET predictions were screened by inputting compound to web-based software https://preadmet.webservice.bmdrc.org/ accessed on 7 January 2024 21.22.

Molecular Docking Calculation

Molecular docking calculation was conducted investigate the binding energy of ligand-receptor complexes and other properties. The targeted protein from the PDB database_https://www.resb.org/) is ID 4EY7. From now on, 31 bioactive compounds derived from Moringa oliefera were retrieved from PubChem (https://pubchem.ncbi.nlm.nih.gov/). The structure of this study was prepared using Chimera 1.14 ²³. The molecules were treated with hydrogen bonds and charged on molecules using residue AMBER FF14SB and another residue, Gasteiger. If all the molecules were prepared, the method validation is a crucial step through redocking. Redocking was performed utilizing rivastigmine as a reference ligand. This drug was located on the active site of the receptor to obtain binding energy and amino acid residue data. Rivastigmine was chosen as a reference ligand because this drug has a half-time in the human body for three hours ²⁴.

Moreover, this drug was accepted by the Food Drug Administration of the United States of America as anti-Alzheimer. Molecular docking calculation was performed using AutoDockTools 1.5.6 with .pdbqt input [16]. Molecular docking calculation was conducted in a grid box of $68 \times 72 \times 68$ with a spacing of 0.375 Å using 100 runs of Lamarckian Genetic Algorithm 25 . The complexes of molecular docking results were visualized using Biovia Discovery Studio to obtain amino acid residue on the active site collect residue amino acids 26 . The complexes of molecular docking results were visualized using Biovia Discovery Studio to obtain amino acid residue on the active site.

13

Molecular Dynamic Simulation

The molecular dynamics simulation protocol was performed of the ligand-AChE complex, which resulted from molecular docking calculations. The ligand is pterygospermin, with lower binding energies than the control ligand. Next, the molecular dynamics simulation results were compared with the molecular dynamics of the control ligand, namely the rivastigmine-AChE complex. A simulation was performed using the YASARA Dynamic Program developed by Bioscience GmBH, Vienna, Austria²⁷. The first step was to input each sample into the program through Option. Then, Macro & Movie menus were selected, and the Set Target was selected as the last step. The temperature and pH of the physiologic were 310K and 7.4 K, respectively.

Furthermore, input macro was performed to conduct molecular lynamic simulation using a prepared sample. In the next step, a running time was set on macro md_run of 50,000 ps (50 ns). This simulation utilized forcefield AMBER14, and the snapshot was kept every 25 ps. The analysis of potential energy, number of hydrogen bonds in the solute, number of hydrogen bonds between solute and solvent, RMSD, and radius of gyration were obtained by unning a macro md_analyze. The analysis of RMSF was carried out with macro md_analyzeres, while the Molecular Mechanics Poisson-Boltzmann Surface Area (MMPBSA) used macro md_analyzebindenergy.

3. RESULTS AND DISCUSSION

Lipinski's Rules of Five and ADMET Studies

Lipinksi's Rule of Five determines and identifies a new drug candidate through permeability and absorption properties ²². Furthermore, this screening step is performed to obtain the physical-chemical properties of the drug candidates (drug-likeness). The rules are molecular mass 3100 Da, hydrogen bond donor lesser than 5, hydrogen bond acceptor lesser than 10, and 21 logP ≤5. The results of Lipinski's Rule of Five of bioactive compounds from *Moringa oleifera* are listed in **Table 1**.

The result of Lipinski's Rule of Five was adhered by seven compounds from moringa leaves (Moringa oliefera), namely beta carotene, lupeol acetate, sitogluside, tocopherol, chlorogenic acid, beta-sitosterol, and myricetin (see Table 1). Beta carotene and sitogluside have a molecular mass of more than 500 Da, which causes the distribution failure to the cell membrane when oral medication is administered. Vice versa, the adherence of the bioactive compounds to Lipinski's Rule of Five simplifies the distribution and penetrates the drug into the cell membranes. Meanwhile, MlogP relates to the hydrophobicity or lipophilicity of a drug candidate. The bioactive compound with a higher MlogP value tends to have hydrophobic properties. It leads to toxicity to the human body because the drug diffuses spreadly and is long regined in a lipid bilayer. Last, the violation of HBD lesser than ≤5 causes absorption difficulties of the drugs in the human body. Based on Lipinski's Rule of Five screening, all 18 bioactive compounds from Moringa oliefera unviolate the rules.

ADMET analysis aims to explore the pharmacokinetics and toxicity of drug candidates from moringa leaves that are orally consumed. Poor pharmacokinetics and toxicity are the primary sources of failure in drug development. In vitro research can be carried out more quickly, but the research results often need to match the in vivo results. In vivo research yields valuable results, but it is time-consuming and costly. Therefore, the in silico method is present to complement these data because it is fast and inexpensive ²⁸. This parameter predicts drug performance to reach the target in the human body (see **Table 2**).

The drug absorption prediction was tested using %HIA and Caco-2 cells. The value of %HIA shows the ability of drug candidate absorption in the human intestine. Data in **Table 2** explained that most ADMET tests were in the 70-100 range, indicating they are well absorbed in the human body ²⁰. Moreover, Caco-2 cell modeling was conducted to predict the absorption ability of bioactive compands through the oral route in vitro. The distribution property of drugs in the human body is seen from the Blood-Brain Barrier (BBB) and Plasma Protein Binding (PPB).

Table 1. Lipinski's Rule of Five of bioactive compound from moringa leaves (*Moringa oleifera*)

				10			
No	Compounds	Lipinski's Rule of Five					
		Molecular Mass 500 (DA)	MlogP 5	Hydrogen Bond Acceptor (HBA) 10	Hydrogen Bond Donor (HBD) 5	Violation of Lipinsksi	Druglike
1	Rivastigmine			Control			
2	1,3 Dibenzil Urea	279	-0.41	6	3	0	Unviolate
3	28 Naftokuinon	158	1.621	2	0	0	Unviolate
4	Beta Carotene	536	12.605	0	0	2	Violate
5	Caffeic Acid	180	1.195	4	3	0	Unviolate
6	Chlorogenic Acid	354	-0.645	9	6	1	Violate
7	Ellagic Acid	302	1.241	8	4	0	Unviolate
8	Gamma Amino Butyric	103	-0.190	3	3	0	Unviolate
9	Kaempferol	286	2.305	6	4	0	Unviolate
10	Lupeol Asetat	468	8.595	2	0	1	Violate
11	Niazimin	399	0.874	8	2	0	Unviolate
12	Niazirin	279	-0.041	6	3	0	Unviolate
13	Pterygospermin	406	4.139	4	0	0	Unviolate
14	Quercetin	302	2.010	7	5	0	Unviolate
15	Sitogluside	576	5.849	6	4	2	Violate
16	Tocopherol	430	8.840	2	1	1	Violate
17	Beta Sitesterol	414	8.024	1	1	1	Violate
18	Vanilin	152	1.213	3	1	0	Unviolate
19	Glucocochlearin	375	-0.220	10	5	0	Unviolate
20	Myricetin	318	1.716	8	6	1	Violate
21	Genistein	270	2.415	5	5	0	Unviolate
22	Moringyne	312	-0,739	7	4	0	Unviolate
23	Rhamnetin	316	2.313	7	4	0	Unviolate
24	Apigenin	270	2.419	5	3	0	Unviolate
25	Daizein	254	2.713	4	2	0	Unviolate
26	Ferulic Acid	194	1.498	4	2	0	Unviolate

The PBB parameter is crucial in the drug design of anti-Alzheimer drugs because this test estimates the drug candidate's ability to relate to the central nervous system (CNS). A drug must reach the CNS and pass the BBB ¹⁹. The function of BBB is to act as a barrier between systemic circulation and CNS, and the function of the barrier is to protect the brain ²⁹. In **Table 2**, in general bi, active compounds from moringa leaves show a BBB in the range of 2.0-0.1, and these values exhibit good absorption. Some compounds have BBB lesser than 0.1, which presents poor absorption ²⁰. Furthermore, PPB is described in percentage, whereas a value more significant than >90% indicates that the drug is bound chemically to blood plasma. PPB also gives information about efficacy and drug disposition.

Furthermore, the drug metabolism element involves the enzym₃₂ cytochrome P450 (CYP450), increasing drug solubility in the human body. The drugs consumed can act as substrates, inhibitors, and inducers. The CYP450 enzymes that play the most role in drug metabolism are CYP3A4 and CYP2D6 ³⁰. CYP3A4 is found primarily in the liver, kidney, ang, brain, endothelium, placenta, and lymphocytes, while CYP2D6 is found in the liver, brain, and heart ²⁸. Based on **Table 2**, it can be seen that most of the compounds originating from Moringa oleifera are predicted to be non-inhibitory against CYP2D6. In CYP3A4, most compounds from Moringa oleifera are inhibitors. **Table 2** describes the toxicity prediction of the extracted compounds from moringa leaves as anti-alzheimer ^{20,31,32}. Most drug candidates are mutagen, and it causes a DNA mutation.

Table 2. ADMET test of bioactive compounds from moringa leaves (Moringa oleifera)

	Compounds		Adsorption		Distribution	oution	Metabolisme, Excretion	e, Excretion		Toxicity	
		%HIA	Caco-2 (nm/sec)	MDCK	BBB	%PPB	CYP 3A4 Inhibition	CYP 2D6 Inhibition	Ames Test Muteuenicity	Mouse Carcinogenicity	Rat Carcinogenicity
-	Rivastigmine	97.95	55.51	0.87	80.0	79.83	Non	Inhibitor	Mutagen	Negative	Negative
2	1,3 Dibenzil Urea	92.80	21.31	41.99	2.95	99.73	Non	Inhibitor	Mutagen	Positive	Negative
3	1,4 Naftokuinon	99.52	20.90	60.05	1.78	68.54	Inhibitor	Non	Mutagen	Negative	Positive
4	Ascorbic Acid	33.15	2.48	0.88	0.11	5.30	Inhibitor	Non	Mutagen	Negative	Negative
5	Ellagic Acid	61.39	20.48	17.29	0.32	88.40	Inhibitor	Non	Mutagen	Negative	Positive
9	Gamma Amino Butyric	73.32	18.02	4.04	0.24	24.75	Inhibitor	Non	Utagen	Positive	Negative
7	Kaempferol	79.43	9.57	79.43	0.28	89.60	Inhibitor	Non	Mutagen	Negative	Positive
8	Niazimin	73.16	19.71	2.25	0.02	56.23	Non	Non	Mutagen	Negative	Negative
6	Niazirin	75.22	0.84	37.24	0.03	48.12	Non	Non	Mutagen	Negative	Negative
10	Ptery gospermin	97.82	5.4.49	0.08	0.05	94.06	Non	Inhibitor	Non-mutagen	Positive	18 ative
Ξ	Quercetin	63.48	3.41	13.35	0.17	93.23	Inhibitor	Non	Mutagen	Negative	Positive
12	Vanillin	93.05	19.59	122.18	0.56	63.14	Inhibitor	Non	Mutagen	Negative	Positive
13	Glucocochlearin	11.99	0.336	17.02	0.08	21.33	Inhibitor	Non	Mutagen	Negative	Positive
14	Genistein	88.12	5.74	39.43	0.17	89.73	Inhibitor	Non	Mutagen	Negative	Positive
15	Moringyne	62.99	13.59	65.99	0.10	46.04	Non	Non	Mutagen	Negative	Negative
16	Rhamnetin	66.11	16.11	21.92	0.05	84.98	Inhibitor	Non	Mutagen	Negative	Positive
17	Apigenin	87.31	10.52	44.30	0.59	100.0	Inhibitor	Non	Mutagen	Positive	Positive
18	Daizein	92.64	2.48	42.99	0.93	95.56	In 7 bitor	Non	Mutagen	Negative	Positive
19	Ferulic Acid	09.06	21.11	228.55	0.75	50.41	Non	Non	Mutagen	Negtive	Positive

Molecular Docking Calculation

Molecular docking calculation in this study was started using redocking step both rivastigmine-AChE receptor interaction. The reason for using rivastigmine as a control drug is that it is USA FDA-approved and has a smaller half-life than donepezil. Donepezil is a native ligand of AChE in 4EY7. De binding energy of rivastigmine with the AChE receptor is -7.77 KJ/mol, which is bound by conventional hydrogen bonds to the amino acid residues PHE295 and TYR124 (See Figure 2.B.). In addition, previous research data states that the active site of AChE is divided into three, namely Catalytic active gorge (GLU334, SER203, HIS447), Long narrow aromatic gorge (TRP86, TYR133, ILE451, GLU202, andGLY448), and Peripheral anionic site (TRP286, PHE295, TYR124, ASP74, and SER125) 33. Based on the three active sites of AChE, it is known that PHE295 and TYR124 are included in the active site of the Peripheral anionic site. The three types of AChE receptor active sites can also be used as comparative data for the research results in this study. The RMSD value of redocking the rivastigmine-AChE receptor complex was obtained at 1.68, indicating the method is well-validated (Figure 1) 34. Figure 1 shows a good comparison position for the ligand before and after redocking. Figure 1 shows the carbonyl oxygen atom as the binding atom for the amino acid residue in the AChE receptor's active site. The carbonyl oxygen atoms of both ligands are close together, but the amine group is positioned opposite.

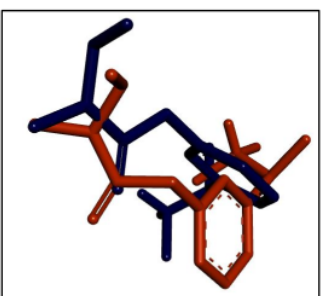


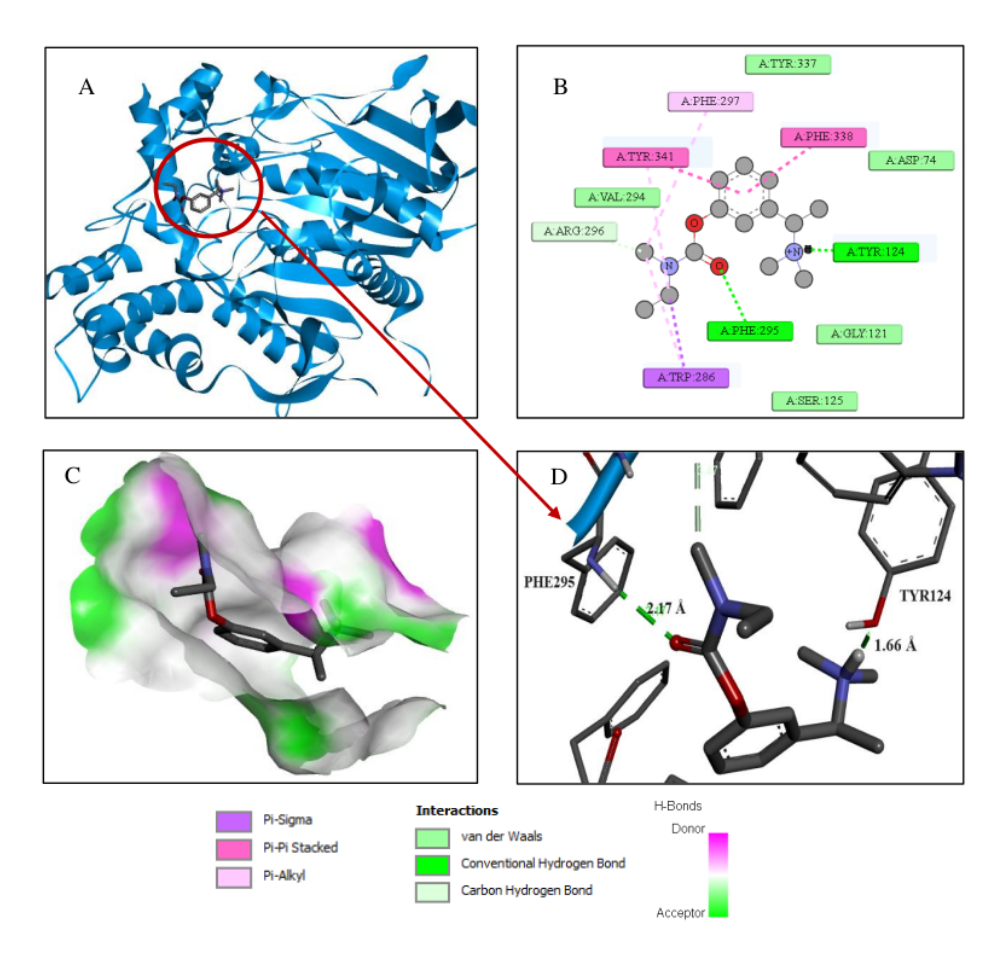
Figure 1. Comparison of rivastigmine in AChE (Dark blue before redocking and orange after redocking)

Table 3 contains 18 Moringa oleifera potential compounds selected from Lipinski's Rule of Five tests. The data proves that ten compounds have lower binding energies than the control ligand, namely 1,3 dibenzyl urea, ellagic acid, niazimin, niazirin, pterygospermine, glucocochlearin, rhamnetin, apigenin, and daidzein. Apart from that, information on inhibition constants (μ M) can also provide significant information in studying ligand inhibitors against a disease. The lower predicted KI value resulting from the calculation indicates that a small concentration is needed to inhibit a receptor ³⁵.

Figure 2 explains in detail the interactions in the rivastigmine+AChE receptor complex. A three-dimensional visualization of the rivastigmine redocking against the AChE receptor is in **Figure 2A**. The control ligand exhibits a conventional hydrogen bond with the amino acid residues TYR124 and PHE295 and linkage with five Van der Wals interactions against TYR337, VAL296, ASP74, GLY121, and SER125. Additionally, amino acid residues TYR341 and PHE338 stacked through π - π interactions. The π -sigma was noticed with TRP289, a carbon-hydrogen bond with ARG296, and PHE297 is π -acyl, respectively (see **Figure 2B**). Conventional hydrogen bond is a primary interaction in molecular docking insight using Autodock Tools. **Figure 2C** exhibits representative hydrogen bonds in the rivastigmine ligand area on the active site of the AChE receptor. The light purple area denotes a donor, while the green area is an acceptor. Amino acid residue PHE295 was linked to the carbonyl oxygen atom (2.17 Å), whereas TYR124 was to the amine rivastigmine group with a band distance of 1.66 Å (**Figure 2.D**). The distance of PHE295 displayed a significant interaction with TYR124 to the active site of the AChE receptor. Therefore, drug candidates from Moringa oleifera were also calculated using a similar method for the AChE receptor to obtain crucial information (seen in **Table 3**). **Table 3** shows that pterygospermine has the lowest binding energy as a potential anti-Alzeimer drug among all the compounds.

Table 3. Molecular docking calculations of bioactive compounds from Moringa leaves against AChE receptors.

No.	Compounds	ID PubChem	Binding Energy	Ki	Conventional hydrogen bond
			(KJ/mol)	constant (µM)	
1	Rivastugmine	77991	-7.77	1.83	PHE295, TYR124
2	1,3 Dibenzil Urea	72889	-8.04	1.29	ASP74
3	1,4 Naftokuinon	8530	-6.31	23.88	PHE338
4	Caffeic Acid	689043	-4.83	287.87	SER203
5	Ellagic Acid	5281855	-7.84	1.82	GLU202, SER203, ASN87, ASP74
6	Gamma Amino Butyric	119	-3.4	1.62	GLY122, SER203, HIS447
7	Kaempferol	5280863	-7.62	1.63	HIS447, TYR341, TYR337, ASP74,
	•				TYR124
8	Niazimin	129556	-8.13	1.09	HIS447
9	Niazirin		-8.10	6.30	GLU202, HIS447, PHE 295
10	Pterygospermin	72201063	-10.28	0.22	TYR133, GLU202
11	Quercetin	5280343	-7.59	2.71	TRP86, GLN71, HIS 447
12	Vaniline		-5.38	113.91	
13	Glucocochlearin	5281135	-9.18	185.10	GLU202, SER203, GLY120, GLY121,
					ALA203, GLY122, HIS447, SER125
14	Genistein	5280961	-8.54	545.94	TYR124, ARG296
15	Moringyne	131751186	-7.73		ASP74, THR83, TYR124
16	Rhamnetin	5281691	-8.9	1.17	ASP74, GLN71
17	Apigenin	5280443	-8.00	91.37	GLU202, GLY120, TYR72
18	Daizein	5391140	-8.47	613.46	GLY122, ARG296, SEER203
19	Ferulic Acid	445858	-5.22	150.29	SER203



Figue 2. 3D visualization of the rivastigmine+AChE receptor complex (A), 2D visualization of the rivastigmine+AChE receptor complex (B), representative hydrogen bonds (C), and atomic interactions between rivastigmine and atoms of the AChE receptor amino acids (D). Apart from that, there is a legend that can explain the interactions that occur.

The potential drug pterygospermine has the lowest binding energy among the 18 compounds in **Table 5**. Based on molecular docking calculations, Pterygospermine has potential as a drug for an anti-Alzheimer alternative. The interaction of the pterygospermine with the AChE receptor is presented in **Figure 3**. The pterygospermine ligand revealed conventional hydrogen bond interactions at amino acid residues TYR133 and GLU202. The mode of interaction of pterygospermine was different from that of the control ligand. However, both amino acid residues were included in the Long narrow aromatic gorge active site of the AChE receptor. Apart from that, ILE451, GLY120, GLY121, ASP74, GLY126, SER125, VAL194, PHE295, PHE297, TYR124, GLY448, and TRP286 exhibited Van der Wals interactions. The linkage π-π stacked was found between TYR341 and TRP86 to pterygospermine. While HIS447, TYR337, and PLE338 were linked to the active site of the ACHhE receptor as carbon-hydrogen bond interactions. In general, the bond distance of amino acid residues in the pterygospermine+AChE receptor complex is longer than the hydrogen bond distance in the rivastigmine+AChE receptor complex. In the pterygospermin-AChE receptor complex, the TYR133 was 2.53 Å to the active site. At the same time, GLU202 has a further distance from the active site in the AChE receptor (2.92 Å).

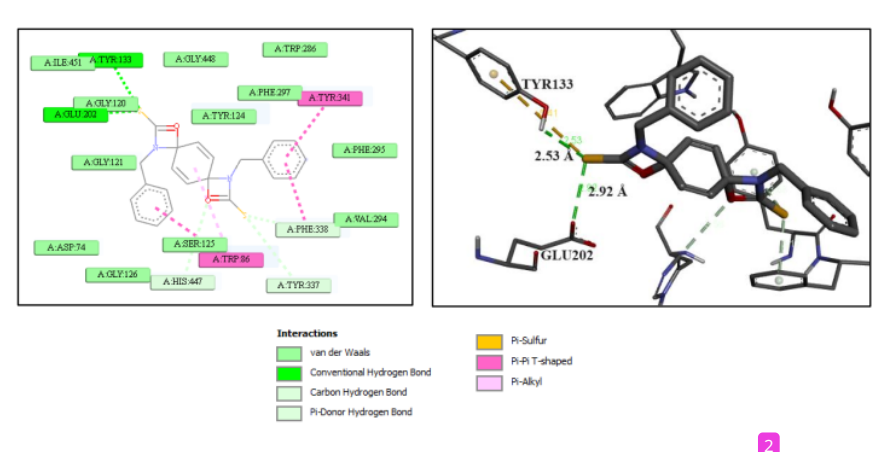


Figure 3. 2D visualization of the pterygospermine+AChE receptor complex (A) and the interaction of the pterygospermine ligand atoms with the amino acid residues of the AChE receptor (B).

Molecular Dynamics Simulation

Molecular dynamic simulation using YASARA Structure is a method to explore the ligand-protein complex's interaction dynamic in physiological conditions of 310K and pH 7.4. The salinity of physiological salt was used at 0.9%. This condition is strong enough to maintain the viability of the two samples. The analysis of potential energy had been obtained after running macro md_analyze. The analysis results from three samples generally showed that an average potential energy significantly increased from 0 ns to 0.5 ns running time (Figure 4). This data showed that the nergy initiation reached energy stability. The energy fluctuation had happened even though the energy reached a stable potential energy (equilibrium phase). Increased energy fluctuation refers to the bonding strength of molecules, while the relaxation of molecular bonds causes decreased energy.

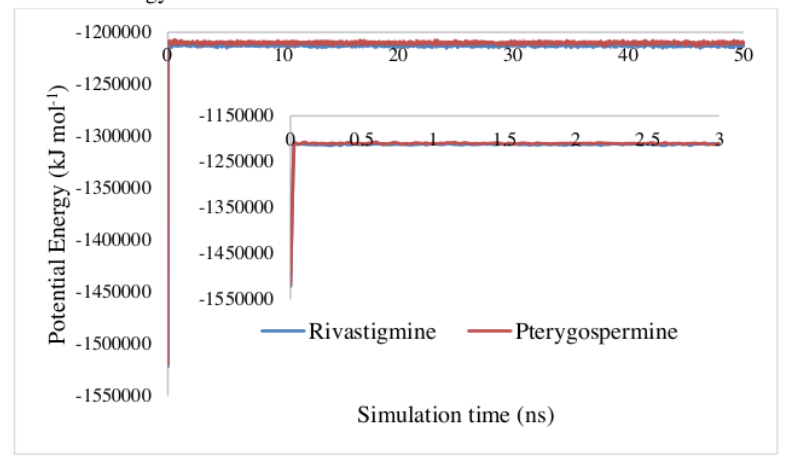


Figure 4. Potential energy of protein-ligand complex at 3 ns and 50 ns (blue line: rivastigmine and red line: pterygospermine)

Furthermore, MMPBSA analysia from rivastigmine showed that the energy average of the implicity solute during running 50 ns is 6.850 kJ mol⁻¹ and for pterygospermine is 37.377 kJ mol⁻¹, respectively (**Table 4**). The MMPBA calculation was performed based on the number of gas phase energy, free energy solvation, and configuration of solute entropy ³⁶. MMPBSA analysis is calculated using **Eq. 1**. Each average energy during 50 ns is shown in **Table 4**.

 $BindEnergy = EpotRecept + EsolvRecept + EpotLigand + EsolvLigand - EpotComplex - EsolvComplex [kJ mol^{-1}]$

Table 4. Components from MMPBSA equation

Energy	Rivastugmine	Pterygospermin
	Average	Average
EpotRecept	-34265.211	-34255.981
EsolvRecept	-24426.497	-24565.717
EpotLigand	32.802	-88.564
EsolvLigand	-30.286	124.030
EpotComplex	-34265.220	-34255.983
EsolvComplex	-24430.822	-24567.627
BindEnergy [kJ/mol]	6.850	37.377

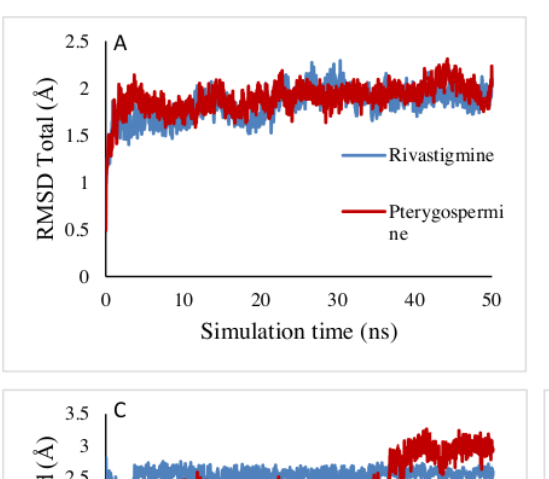
Total MSD, RMSF, Ligand Configuration, and Radius of Gyration

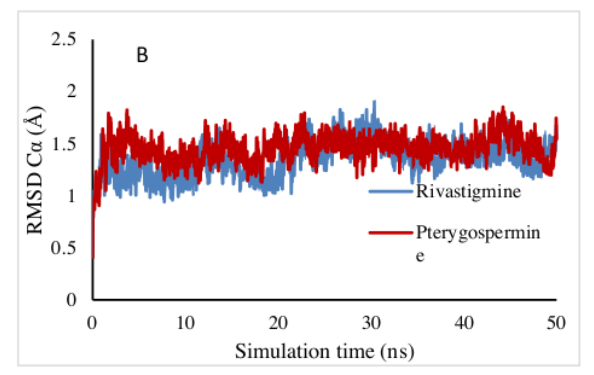
Root Mean Square Deviation (RMSD) is analysis score that provides conformation changes in macromolecules. This analysis also to predict the stability of ligand-protein combination in this study. Macromolecules act as receptors after an interaction with specific ligands. The RMSD analysis is obtained after running macro md_analyze. RMSD is also used as a deviation standard of conformation change. The value of RMSD is < 2Å generally applied to docking results ³⁷. RMSD data represents sample stability in simulation conditions where the conformation change is insignificant to dynamic stability. The meaning of dynamic stability is the absence of significant conformational changes, which is better known as the unfolding process.

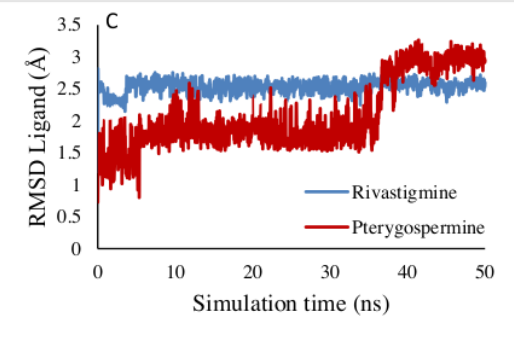
On the other hand, certain receptors resulting from the simulation have an RMSD of 3 Å, so this receptor system experiences significant conformation change from the native condition. **Figure 5A** shows the RMSD values for both stable samples with some fluctuations. Moreover, total RMSD of two samples revealed an average value of 2 Å, so the protein conformation in two samples was predicted not to change significantly.

The RMSD of the C-alpha protein for both samples was lower than the total RMSD value in **Figure 5B**. However, the Pterygospermin ligand showed an RMSD value that was not significantly different from that of rivastigmine as a positive control, indicating the potential nature of Ptgygospermin as an AChE inhibitor. In addition to the RMSD of the entire molecule, the YASARA program can also be used to view the RMSD of the ligand configuration. The RMSD ligand analysis indicated that the ligand in the Rivastigmine complex is much more stable during the simulation time of 50 ns, with a range of 2-2.5 Å. Besides that, the pterygospermin ligand exhibited different dynamics than the rivastigmine ligand. At the initial simulation at 0-35 ns, RMSD of the pterygospermine ligand was lower than the rivastigmine ligand. However, the system of the rivastigmine ligand experienced quite significant changes. This change was a significant conformational change, which induced the RMSD of the ligand to increase, ranging from 3-3.5 Å (**Figure 5C**). This condition can support the binding energy data, where pterygospermin has a more positive energy value than rivastigmine due to conformational changes in the pterygospermin ligand structure.

Radius of gyration (RG) analysis describes the equilibrium conformation of the entire simulation system. The RG value can also be explained as the radius of rotation of the dynamic povement of a protein-protein or protein-compound complex towards the solvent, so it is one way to predict the singlation of sample solubility in a solution or liquid solvent 38. The lowest value indicates the folded condition of the protein, while the highest value indicates the conformational condition of the protein when it is unfolded 39. The comparison results between the complexes show that the docking of the rivastigmine and pterygospermine ligands did not significantly change the RG pattern or that the protein was folded during the simulation time (Figure 5D).







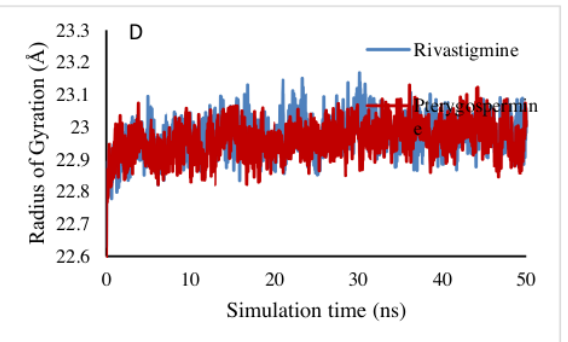


Figure 5. RMSD of rivastigmine and pterygospermin complexes to AChE (A), RMSD Cα of rivastugmine and pterygospermin complexes to AChE (B), RMSD of ligand configuration (C), dan Comparison of RG patterns between rivastigmine and pterygospermin complexes with AChE (D)

RMS analysis of amino acid residue

Root Mean Square Fluctuation (RMSF) provides more detailed information on conformational changes because it it elated to fluctuations at the level of amino acid and nucleotide residues of the ligand. The RMSF results of the amino acid residues of the AChE protein structure in the rivastigmine and pterygospermine complexes show an average value of around 2 Å. In **Figure 6**, it can be seen that several amino acid residues have RMSF values that exceed 3 Å, so it is predicted that bond relaxation occurred in the target protein conformation, especially several residues with RMSF values above 4 Å.

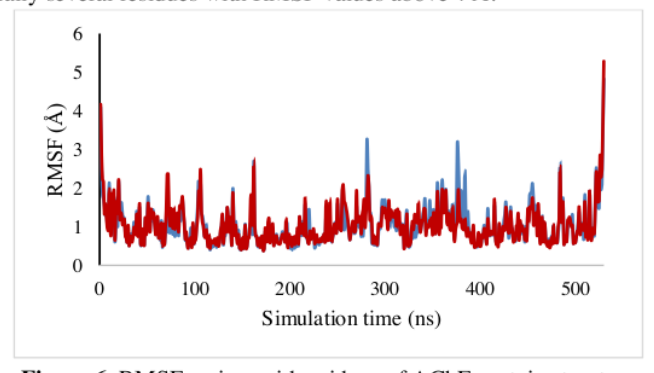


Figure 6. RMSF amino acid residues of AChE protein structure

4. CONCLUSIONS

Study of bioactive compounds from *Moringa oleifera* to AChE have been successfully investigated using ADMET properties, molecular docking, and molecular dynamics. The results of the screening stage obtained eighteen bioactive compounds for molecular docking calculations. Pterygospermine produces the lowest binding energy with hydrogen bond interactions at amino acid residues TYR133 and GLU202 in the active AChE site. A comparison of pterygospermine+AChE and rivastigmine+AChE complexes was simulated through molecular dynamics. The results of the comparison of the AChE complex with rivastigmine and pterygospermine show that the pterygospermine ligand has a stable interaction with AChE like the positive control (rivastigmine) against AChE based on RMSD and RMSF data. The Radius of Gyration analysis results do not show that the addition of ligands can cause an unfolded effect on the protein. Based on the data, rivastigmine's binding energy is better than pterygospermine's because of the change in the conformation of the pterygospermine ligand during the simulation time.

Acknowledgement

The author thanks Hafiz Aji Aziz for valuable discussions

BIBLIOGRAPHY

- Karran E, De Strooper B. The amyloid hypothesis in Alzheimer disease: new insights from new therapeutics. Nat Rev Drug Discov. 2022;21(4):306-318. doi:10.1038/s41573-022-00391-w
- Pitchai A, Rajaretinam RK, Mani R, Nagarajan N. Molecular interaction of human acetylcholinesterase with trans-tephrostachin and derivatives for Alzheimer's disease. Heliyon. 2020;6(9):e04930. doi:10.1016/j.heliyon.2020.e04930
- Anonymous. Symptoms of Alzheimer's disease.
- Kuzu B, Tan M, Taslimi P, Gülçin İ, Taşpınar M, Menges N. Mono- or di-substituted imidazole derivatives for inhibition of acetylcholine and butyrylcholine esterases. *Bioorg Chem.* 2019;86(October 2018):187-196. doi:10.1016/j.bioorg.2019.01.044
- Wang L, Moraleda I, Iriepa I, et al. 5-Methyl-: N -(8-(5,6,7,8-tetrahydroacridin-9-ylamino)octyl)-5 H -indolo[2,3-b] quinolin-11-amine: A highly potent human cholinesterase inhibitor. *Medchemcomm*. 2017;8(6):1307-1317. doi:10.1039/c7md00143f
- Malik YA, Awad TA, Abdalla M, et al. Chalcone Scaffolds Exhibiting Acetylcholinesterase Enzyme Inhibition: Mechanistic and Computational Investigations. *Molecules*. 2022;27(10):1-17. doi:10.3390/molecules27103181
- Ghimire S, Subedi L, Acharya N, Gaire BP. Moringa oleifera: A Tree of Life as a Promising Medicinal Plant for Neurodegenerative Diseases. J Agric Food Chem. 2021;69(48):14358-14371. doi:10.1021/acs.jafc.1c04581
- Misra AB and L. Ayurvedic Plants in Brain Disorders: The Herbal Hope. J Tradit Med Clin Naturop. 2017;06(02):1-9. doi:10.4172/2573-4555.1000221
- Rats MS treated, Djiogue S, Kammogne IY, Etet S, Kavaye AK, Zemo F. Neuroprotective Effects of the Aqueous Extract of Leaves of Moringa oleifera Neuroprotective Effects of the Aqueous Extract of Leaves of Moringa oleifera (Moringaceae) in Scopolamine-Treated Rats. 2022; (June). doi:10.35248/0974-8369.22.14.474
- Rats MS treated, Djiogue S, Kammogne IY, Etet S, Kavaye AK, Zemo F. Neuroprotective Effects of the Aqueous Extract of Leaves of Moringa oleifera Neuroprotective Effects of the Aqueous Extract of Leaves of Moringa oleifera (Moringaceae) in Scopolamine-Treated Rats. Biol Med. 2022;14(2):1-5. doi:10.35248/0974-8369.22.14.474
- Magaji UF, Sacan O, Yanardag R. Antilipase, antiacetylcholinesterase and antioxidant activities of Moringa oleifera extracts. Rom All rights Reserv Rom Biotechnol Lett. 2022;27(1):3208-3214. doi:10.25083/rbl/27.1/3208-3214
- Azlan UK, Khairul Annuar NA, Mediani A, et al. An insight into the neuroprotective and anti-neuroinflammatory effects and mechanisms of Moringa oleifera. Front Pharmacol. 2023;13(January):1-18. doi:10.3389/fphar.2022.1035220
- Kou X, Li B, Olayanju JB, Drake JM, Chen N. Nutraceutical or pharmacological potential of Moringa oleifera Lam. Nutrients. 2018;10(3). doi:10.3390/nu10030343
- Amat-Ur-rasool H, Ahmed M, Hasnain S, Ahmed A, Carter WG. In Silico Design of Dual-Binding Site Anti-Cholinesterase Phytochemical Heterodimers as Treatment Options for Alzheimer's Disease. Curr Issues Mol Biol. 2022;44(1):152-175. doi:10.3390/cimb44010012
- Rocchetti G, Pagnossa JP, Blasi F, et al. Phenolic profiling and in vitro bioactivity of Moringa oleifera leaves as affected by different extraction solvents. Food Res Int. 2020;127(June 2019). doi:10.1016/j.foodres.2019.108712
- 16. Mahaman YAR, Huang F, Wu M, et al. Moringa Oleifera Alleviates Homocysteine-Induced Alzheimer's

- Disease-Like Pathology and Cognitive Impairments. J Alzheimer's Dis. 2018;63(3):1141-1159. doi:10.3233/JAD-180091
- Manogna C, Margesan T. In silico and pharmacokinetic studies of glucomoring in from Moringa oleifera root for Alzheimer's disease like pathology. 2024;(September 2021). doi:10.2144/fsoa-2023-0255
- Grinter SZ, Zou X. Challenges, applications, and recent advances of protein-ligand docking in structure-based drug design. *Molecules*. 2014;19(7):10150-10176. doi:10.3390/molecules190710150
- Farihi A, Bouhrim M, Chigr F, et al. Exploring Medicinal Herbs' Therapeutic Potential and Molecular Docking Analysis for Compounds as Potential Inhibitors of Human Acetylcholinesterase in Alzheimer's Disease Treatment. Med. 2023;59(10). doi:10.3390/medicina59101812
- Kiruthiga N, Alagumuthu M, Selvinthanuja C, Srinivasan K, Sivakumar T. Molecular Modelling, Synthesis and Evaluation of Flavone and Flavanone Scaffolds as Anti-inflammatory Agents. Antiinflamm Antiallergy Agents Med Chem. 2020;20(1):20-38. doi:10.2174/1871523019666200102112017
- Nainwal LM, Shaququzzaman M, Akhter M, et al. Synthesis, ADMET prediction and reverse screening study of 3,4,5-trimethoxy phenyl ring pendant sulfur-containing cyanopyrimidine derivatives as promising apoptosis inducing anticancer agents. *Bioorg Chem*. 2020;104:104282. doi:10.1016/j.bioorg.2020.104282
- Lipinski CA, Lombardo F, Dominy BW, Feeney PJ. Experimental and computational approaches to estimate solubility and permeability in drug discovery and development settings. Adv Drug Deliv Rev. 2012;64(SUPPL.):4-17. doi:10.1016/j.addr.2012.09.019
- Pettersen EF, Goddard TD, Huang CC, et al. UCSF Chimera A visualization system for exploratory research and analysis. J Comput Chem. 2004;25(13):1605-1612. doi:10.1002/jcc.20084
- Ghazal TM, Abbas S, Munir S, et al. Alzheimer disease detection empowered with transfer learning. Comput Mater Contin. 2022;70(3):5005-5019. doi:10.32604/cmc.2022.020866
- Morris GM, Goodsell DS, Halliday RS, et al. Automated docking using a Lamarckian genetic algorithm and an empirical binding free energy function. J Comput Chem. 1998;19(14):1639-1662. doi:10.1002/(SICI)1096-987X(19981115)19:14<1639::AID-JCC10>3.0.CO;2-B
- Gaarett M. Morris, Ruth Huey, William Lindstrom, Michel F. Sanner, Richard K. Belew, Davi S. Goodsell AJO. AutoDock4 and AutoDock Tools4: Automated Docking with Selective Receptor Flexibility. *J Comput Chem*. 2012;32:174-182. doi:10.1002/jcc
- Humble HL and MS. YASARA: A Tool to Obtain Structural Guidance in Biocatalytic Investigations. Protein Eng. 2017;1685:43-67.
- Shin HK, Kang Y mook, No KT. Predicting ADME Properties of Chemicals Predicting ADME Properties of Chemicals. In:: 2017; Shin, H. K., Kang, Y. M., No, K. T. (2017). Pred. doi:10.1007/978-3-319-27282-5
- Daina A, Zoete V. A BOILED-Egg To Predict Gastrointestinal Absorption and Brain Penetration of Small Molecules. ChemMedChem. Published online 2016:1117-1121. doi:10.1002/cmdc.201600182
- Lynch T, Price A. The effect of cytochrome P450 metabolism on drug response, interactions, and adverse effects. *Am Fam Physician*. 2007;76(3):391-396.
- Ajala A, Eltayb WA, Abatyough TM, et al. In-silico Screening and ADMET evaluation of Therapeutic MAO-B Inhibitors against Parkinson Disease. *Intell Pharm*. 2023;(November 2023). doi:10.1016/j.ipha.2023.12.008
- Rasyid H, Soekamto NH, Firdausiah S. Cinnamamide Derivatives as Anticancer Agent: Study of Molecular Docking, Molecular Dynamic Simulation, and ADMET Properties. *Malaysian J Chem.* 2023;25(5):160-167. doi:10.55373/mjchem.v25i5.160
- Peitzika SC, Pontiki E. A Review on Recent Approaches on Molecular Docking Studies of Novel Compounds Targeting Acetylcholinesterase in Alzheimer Disease. *Molecules*. 2023;28(3). doi:10.3390/molecules28031084
- 34. J Comput Chem 2007 Huey A semiempirical free energy force field with charge-based desolvation.pdf.
- Raeisi S. Molecular docking approach of monoamine oxidase B inhibitors for identifying new potential drugs: Insights into drug-protein interaction discovery, 2013;5:24-34.
- Aldeghi M, Bodkin MJ, Knapp S, Biggin PC. Statistical Analysis on the Performance of Molecular Mechanics Poisson-Boltzmann Surface Area versus Absolute Binding Free Energy Calculations: Bromodomains as a Case Study. J Chem Inf Model. 2017;57(9):2203-2221. doi:10.1021/acs.jcim.7b00347
- Arthur TO and O. Software News and Updates Gabedit A Graphical User Interface for Computational Chemistry Softwares. J Comput Chem. 2012;32:174-182. doi:10.1002/jcc
- Lobanov MY, Bogatyreva NS, Galzitskaya O V. Radius of gyration as an indicator of protein structure compactness. Mol Biol. 2008;42(4):623-628. doi:10.1134/S0026893308040195
- Yamamoto E, Akimoto T, Mitsutake A, Metzler R. Universal Relation between Instantaneous Diffusivity and Radius of Gyration of Proteins in Aqueous Solution. Phys Rev Lett. 2021;126(12):1-20. doi:10.1103/PhysRevLett.126.128101

ORIGINA	ALITY REPORT			
SIMILA	2% ARITY INDEX	10% INTERNET SOURCES	8% PUBLICATIONS	1% STUDENT PAPERS
PRIMAR	Y SOURCES			
1	WWW.NC	bi.nlm.nih.gov		2%
2	WWW. M Internet Sour			1 %
3	japsonli Internet Sour			1 %
4	innovar Internet Sour	eacademics.in		1 %
5	Benlyas Bouachi benzodi targetin	elhassan, Hanar , Tahar Lakhlifi, rine. "Study of r azepine analog g by molecular ies prediction",	Mohammed novel triazolo-ues as antidep docking and A	ressants
6	www2.r	ndpi.com ce		1 %
7	assets.r Internet Sour	esearchsquare.	com	<1%

Therapeutic MAO-B Inhibitors against Parkinson Disease", Intelligent Pharmacy, 2023

Publication

Alaa Alnoor Alameen, Mohnad Abdalla, 12 Hanan M. Alshibl, Monerah R. AlOthman et al. "In-silico studies of glutathione peroxidase4 activators as candidate for multiple sclerosis management", Journal of Saudi Chemical Society, 2022

<1%

Publication

Esslali Soukaina, Nabil Al-Zaqri, Ismail Warad, Hamza Ichou, Koubi Yassine, Farhate Guenoun, Mohammed Bouachrine. "Novel antiproliferative inhibitors from salicylamide derivatives with dipeptide moieties using 3D-QSAR, molecular docking, molecular dynamic simulation and ADMET studies", Journal of Molecular Structure, 2023

<1%

Publication

Fabio Carniato, Marco Ricci, Lorenzo Tei, Francesca Garello et al. "Novel Nanogels Loaded with Mn(II) Chelates as Effective and Biologically Stable MRI Probes", Small, 2023

<1%

Joyce Oloaigbe Ogidigo, Chioma Assumpta Anosike, Parker Elijah Joshua, Collins U. Ibeji et al. "UPLC-PDA-ESI-QTOF-MS/MS fingerprint of purified flavonoid enriched fraction of; antioxidant properties, anticholinesterase activity and in studies ", Pharmaceutical Biology, 2021 <1%

Sow Tein Leong, Sook Yee Liew, Kooi Yeong Khaw, Hazlina Ahmad Hassali et al. "13C NMR-based dereplication using MixONat software to decipher potent anticholinesterase compounds in Mesua lepidota bark", Bioorganic Chemistry, 2023

<1%

17	dergipark.org.tr Internet Source	<1%
18	legalservicesboard.org.uk Internet Source	<1%
19	www.derpharmachemica.com Internet Source	<1%
20	Dušan Petrović, Ansgar Bokel, Matthew Allan, Vlada B. Urlacher, Birgit Strodel. "Simulation- Guided Design of Cytochrome P450 for Chemo- and Regioselective Macrocyclic Oxidation", Journal of Chemical Information and Modeling, 2018 Publication	<1%
21	Rizal Irfandi, Indah Raya, Ahyar Ahmad, Ahmad Fudholi et al. "Anticancer potential of Cu(II)prolinedithiocarbamate complex: design, synthesis, spectroscopy, molecular docking, molecular dynamic, ADMET, and in- vitro studies", Journal of Biomolecular Structure and Dynamics, 2023 Publication	<1%
22	Sundarapandian Thangapandian, Shalini John, Sugunadevi Sakkiah, Keun Woo Lee.	<1%

"Molecular modelling study on human

histamine H1 receptor and its applications in

virtual lead identification for designing novel inverse agonists", Molecular Simulation, 2011

Publication

23	Yi Kuang, Xiaodong Ma, Wenjing Shen, Qingqing Rao, Shengxiang Yang. "Discovery of 3CLpro inhibitor of SARS-CoV-2 main protease", Future Science OA, 2023 Publication	<1%
24	pharmacologyonline.silae.it Internet Source	<1%
25	pubmed.ncbi.nlm.nih.gov Internet Source	<1%
26	tbiomed.biomedcentral.com Internet Source	<1%
27	www.dovepress.com Internet Source	<1%
28	www.healthproductsdistributors.com Internet Source	<1%
29	www.researchgate.net Internet Source	<1%
30	www.scirp.org Internet Source	<1%
31	Dikdik Kurnia, Salsabila Aqila Putri, Sefren Geiner Tumilaar, Achmad Zainuddin, Hendra Dian Adhita Dharsono, Meiny Faudah Amin. "In silico Study of Antiviral Activity of	<1%

Polyphenol Compounds from Ocimum basilicum by Molecular Docking, ADMET, and Drug-Likeness Analysis", Advances and Applications in Bioinformatics and Chemistry, 2023

Publication

Ward, Michael B, Michael J Sorich, Allan M Evans, and Ross A McKinnon. "Cytochrome P450 Part 3: Impact of Drug-Drug Interactions", Journal of Pharmacy Practice and Research, 2009.

<1%

Publication

Arwansyah Arwansyah, Abd Farid Lewa,
Muliani Muliani, Siti Warnasih, Apon Zaenal
Mustopa, Abdur Rahman Arif. " Molecular
Recognition of Active Compounds for Stunted
Growth Prevention Using Network
Pharmacology and Molecular Modeling
Approach ", ACS Omega, 2023

<1%

Hafsa Amat-ur-Rasool, Mehboob Ahmed, Shahida Hasnain, Abrar Ahmed, Wayne Grant Carter. "In Silico Design of Dual-Binding Site Anti-Cholinesterase Phytochemical Heterodimers as Treatment Options for Alzheimer's Disease", Current Issues in Molecular Biology, 2021

<1%

Publication

Publication

35

Mijanur Rahman, Asma Talukder, Rekha Akter. "Computational Designing and Prediction of ADMET Properties of Four Novel Imidazole-Based Drug Candidates Inhibiting Heme Oxygenase-1 Causing Cancers", Molecular Informatics, 2021

<1%

Publication

36

Omer Asghar Dara, Jose Manuel Lopez-Guede, Hasan Issa Raheem, Javad Rahebi, Ekaitz Zulueta, Unai Fernandez-Gamiz. "Alzheimer's Disease Diagnosis Using Machine Learning: A Survey", Applied Sciences, 2023 **Publication**

<1%

Exclude quotes Exclude bibliography On

Off

Exclude matches

Off